Int J Mater Form (2009) Vol. 2 Suppl 1:65–68
DOI 10.1007/s12289-009-0573-y


# Crystal plasticity prediction of Lankford coefficients using the MULTISITE model: influence of the critical resolved shear stresses

**Walid Hammami[1], Laurent Delannay[2,3], Anne Marie Habraken[1,3,*], Laurent Duchêne[1,3]**

[1] Department ARGENCO, Division MS²F, University of Liège,
Chemin des Chevreuils 1, 4000 Liège, Belgium
[2] Department of Mechanical Engineering, Université catholique de Louvain (UCL),
av. G. Lemaître 4, 1348 Louvain-la-Neuve, Belgium
[3] FNRS Fonds de la Recherche Scientifique

**ABSTRACT:** The MULTISITE model [1] is based on polycrystalline plasticity and the underlying hypotheses of the model are (i) that the deformation of each grain is significantly influenced by the interaction with a limited number of adjacent grains, and (ii) that local strains deviate from their macroscopic average according to specific "relaxation modes". The LAMEL model [2] is reformulated into the more general elastic-viscoplastic MULTISITE model permitting various relaxation modes. This model has been validated for cubic materials but hexagonal close-packed (HCP) crystals usually demonstrate larger anisotropy than cubic crystals. The model was used to simulate uniaxial tensile tests performed on rolled sheets made of Ti-6Al-4V. The Lankford coefficients (r) calculated in various directions in the plane of the sheet were analysed. In this study, different grain interaction hypotheses were tested. Besides, it appeared that the value of the critical resolved shear stresses (CRSS) of the different slip system families of the HCP metal had significant effects on the results. Their influence as well as the influence of the strain rate sensitivity parameter was examined.

**KEYWORDS:** Lankford coefficient, Anisotropy, CRSS, Texture, TA6V

## 1 INTRODUCTION

Some authors have worked on the identification of the active slip systems in TA6V and their Critical Resolved Shear Stresses (CRSS). Only the α–phase is simulated in their modelling approaches. A consensus among the authors exists on the type of slip encountered during plastic deformation of TA6V. However, very different values can be found in the literature for the relative CRSS among the slip system families. In this respect, a sensitivity study of the CRSSs on the mechanical anisotropy (regarding the Lankford coefficients) of the studied Titanium alloy was investigated using various crystal plasticity models such as Taylor and ALAMEL.

## 2 MATERIAL

The TA6V is a dual phase alloy (α+β) having a main α matrix (hexagonal crystal lattice) and a secondary β phase (body centred cubic), which does not exceed 8% in volume fraction. Both phases show the same hardness at room temperature. These two phases present cold rolling textures which is called type III or L-Type textures (Longitudinal) [3].
Rolled sheets of TA6V presents a complex texture with three main peaks on the (00.2) pole figure (PF): two components whose c axes are almost in TD (these components resulting from hot rolling) and one central component with two peaks at 20° to ND in the ND-RD plane. This latter component results from cold rolling [4]. The second β phase is spread almost homogeneously and its average grain size ranges from 2 to 3 μm.

### 2.1 DEFORMATION MECANISMS

At the beginning of the plastic deformation, the following glide systems are observed in decreasing order of contribution in TA6V [5]:

- Prismatic glide (10.0) <11.0>
- Basal glide (00.2) <11.2>
- Pyramidal <c+ a> glide (10.1) <11.3>.

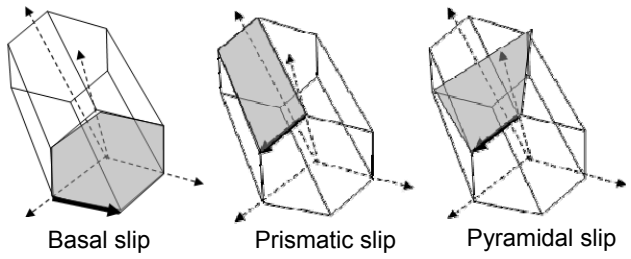


***Figure 1:*** Slip planes in HCP cell.

* Corresponding author: anne.habraken@ulg.ac.be

## 3 NUMERICAL SIMULATIONS

Uniaxial tension test simulations for many angles to the Rolling Direction RD (from 0° to 90°) were performed using different models included into the MULTISITE code. The initial texture of the TA6V was used and different values of material parameters were checked as explained hereafter.

### 3.1 CRYSTAL PLASTICITY MODELS

**Full Constraints (FC) Taylor Model:** In this model the microscopic velocity gradient is assumed to be equal to the macroscopic velocity gradient everywhere in the polycrystal.

$$\underline{\underline{L}}^{micro} = \underline{\underline{L}}^{Macro} \tag{1}$$

Therefore, the plastic strain is distributed uniformly among the polycrystalline aggregate. Consequently, the stress equilibrium at the grain boundaries and inside the grains is not necessarily satisfied.

**Classical relaxed constraints model:** According to specific relaxation modes, the microscopic strain rate of each crystal deviates from the macroscopic strain rate. Taking the relaxation modes into account we have

$$\underline{\underline{L}}^{micro} = \underline{\underline{L}}^{Macro} + \dot{\gamma}^{rlx}\,\underline{\underline{L}}^{rlx} \tag{2}$$

The component $\dot{\gamma}^{rlx}\,\underline{\underline{L}}^{rlx}$ in the above equation allows relaxing the component of the velocity gradient corresponding to the chosen micro-macro model. The slip rates $\dot{\gamma}^{rlx}$ (one by relaxation mode) are determined by equilibrium considerations. The matrix $\underline{\underline{L}}^{rlx}$ represents the relaxation mode chosen. In the Lath model, there is only one relaxation mode on the component $L_{13}^{micro}$ and the corresponding $\underline{\underline{L}}^{rlx}$ is expressed in equation (3).

$$\underline{\underline{L}}^{rlx} = \begin{bmatrix} 0 & 0 & 1 \\ 0 & 0 & 0 \\ 0 & 0 & 0 \end{bmatrix} \tag{3}$$

The pancake model is the most popular relaxed constraints model. The relaxation modes are $L_{13}^{micro}$ and $L_{23}^{micro}$. This model is especially adapted to the computation of texture evolution during rolling (with flat and elongated grains).

**Lamel model (multi grain model)**: The deformation textures predicted by the classical relaxed-constraints models are not really much better than those predicted by the Taylor full-constraints model. The suspected reason could be that the local interaction between adjacent grains is not taken into account. This statement led to develop the multi-grain models.

The concept of "cluster of interaction" appears in the multi grain models. In the Taylor model and the classical relaxed-constraints models, the cluster of interaction contains only one grain; they are one-grain models with no interaction between adjacent grains. The multi-grain models use the same relaxation tensors as in the classical relaxed-constraints theories but they assume that the macroscopic velocity gradient is achieved collectively by the cluster of interacting grains. For instance, in the Lamel model (two-grains model), if the grain I interacts with the grain II, it implies that

$$\frac{\underline{\underline{L}}^{micro,I} + \underline{\underline{L}}^{micro,II}}{2} = \underline{\underline{L}}^{Macro} \tag{4}$$

According to equation (4), we can write the velocity gradient of the two grains as a function of the macroscopic velocity gradient (Einstein's summation is applied on rlx index)

$$\begin{aligned} \underline{\underline{L}}^{micro,I} &= \underline{\underline{L}}^{Macro} + \dot{\gamma}^{rlx}\,\underline{\underline{L}}^{rlx} \\ \underline{\underline{L}}^{micro,II} &= \underline{\underline{L}}^{Macro} - \dot{\gamma}^{rlx}\,\underline{\underline{L}}^{rlx} \end{aligned} \tag{5}$$

The relaxation modes used in the Lamel model are identical to those used in the Pancake model because the Lamel model is also especially dedicated to rolling textures (with flattened and elongated grains). The relaxations considered in the cluster are represented in Figure 2.

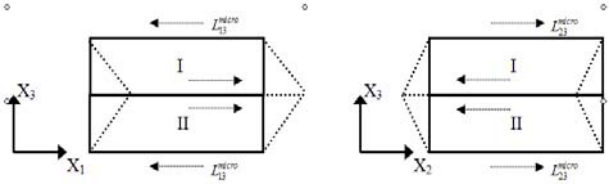


***Figure 2:*** Relaxation of the shear components $L_{13}^{micro}$ and $L_{23}^{micro}$ for a cluster obtained after rolling (Lamel model) $X_1$ = RD, $X_2$ = TD, $X_3$ = ND.

We can notice that the chosen relaxations leave the rolling plane ($X_1$ – $X_2$) undistorted and unrotated (compared to the macroscopic deformation) and that equal and opposite shear stresses are imposed in each grain of the cluster (for each relaxation mode) to achieve a partial equilibrium and ensure a consistent interface. The stress equilibrium (concerning the relaxed components) is assured at the interface of the grains in the cluster without requiring that these shear stresses would be equal to zero as it is done in the classical relaxed-constraints models.

**Alamel model (advanced lamel model):** The Advanced Lamel model is an attempt to solve the problem of the grain shape. Its mathematical description only differs slightly from the Lamel model. In the Lamel model, the interfaces between two adjacent grains must always be parallel to the RD – TD plane. This constraint limits this model to rolling processes. In the recent Advanced Lamel (ALAMEL) model, the orientations of the interfaces are defined

either by the user as a function of the material and the process investigated or they can be randomly chosen with a rule taking into account the grain shape. Therefore, the ALAMEL model is suitable for any deformation mode and different grain shapes (not only flat, elongated grains).

The different options investigated are:

- FC: Full Constraints Taylor model.
- PCK: Relaxed Constraints Taylor (pancake).
- ALAM: ALAMEL with equi-axed grains.
- PSD: ALAMEL with flat grains (deformed by plane strain deformation).
- FIB: ALAMEL with elongated grain's shape.

### 3.2 HARDENING

For the determination of the slip rates, we adopt the viscoplastic expression:

$$\dot{\gamma} = \dot{\gamma}_0 \left| \frac{\tau^\alpha}{\tau_C} \right|^{\frac{1}{m}} sign(\tau^\alpha) \quad (6)$$

In this expression, the reference slip rate $\dot{\gamma}_0$ and the sensitivity exponent *m* are kept constant, whereas the critical resolved shear stress $\tau_C$ increases due to strain hardening. The hardening law selected in the present study assumes an identical $\tau_C$ on all slip systems:

$$\tau_C = \tau_{C0} \left( 1 + \frac{\Gamma_{tot}}{\Gamma_0} \right)^n \quad (7)$$

Where $\tau_{C0}$, $\Gamma_0$ and n are material parameters and

$$\Gamma_{tot} = \int_0^t \sum \alpha \left| \dot{\gamma}_0 \right| dt \quad (8)$$

### 3.3 STUDIED PARAMETERS

Based on the values of CRSSs found in the literature [5][6], we fixed a range for each CRSS, such as basal, prismatic and pyramidal CRSS, in order to sweep all used values by different authors *(Table 1)*. Different values of the strain rate sensitivity (1/m) were also used in the computations.

***Table 1:*** *CRSSs and strain rate sensitivity used during the computations*

| Critical Resolved Shear Stresses | | | Strain rate sensitivity (1/m) |
|---|---|---|---|
| Basal | Prismatic | Pyramidal | |
| 1 | 0.2<br>0.4<br>0.6<br>0.8<br>1<br>1.2 | 1<br>2<br>4<br>6<br>8 | 5<br>10<br>20<br>30 |

To take into account all the combinations of CRSSs and the strain rate sensitivity with each of the five models, the number of computations was 1x6x5x4x5 = 600 simulations. Only a summary of the results is presented hereafter.

## 4 RESULTS AND DICUSSIONS

### 4.1 CRSS EFFECT WITH ALAMEL MODEL

The variation of the T_pyramidal has a great influence on the evolution of the Lankford coefficient (Figure 3). When T-pyramidal increases from 1 to 8, the Lankford coefficient increases by 77% at 45° and by 36% at 90° from RD and there is a low effect at 0° (+5.8%).

***Table 2:*** *Effect of the CRSS's and the strain rate sensitivity on the Lankford coefficients (r)*

| | FC | PCK | ALAM | PSD | FIB |
|---|---|---|---|---|---|
| **T_PRISM** | - Low influence | - T_prism ↑ → r↓ | - Low influence | - T_prism ↑ → r(90°)↓ | - Low effect at 45°<br>- No effect at 0° and 90° |
| **T_PYRAM** | - T_pyram ↑ → r(45°)↑<br>- Low effect at 90° | - At 0° and 90°: T_pyram ↑ → r↓<br>- At 45° depends on S.R. sensitivity and T_prism | - T_pyram ↑ → r(45°)↑<br>- Low effect at 90° | - At 0° and 90°: T_pyram ↑ → r↓<br>- At45°:T_pyram↑ → r↑ | - T_pyram ↑ → r(45°)↑<br>- Low effect at 90° |
| **STRAIN RATE SENSITIVITY (1/m)** | - Increases the T_pyram effect at 45°<br>- Low effect at 0° and 90° | - - | - Increases the T_pyram effect at 45°<br>- Low effect at 0° and 90° | - Low influence | - Increases the T_pyram effect at 45°<br>- Low effect at 0° and 90° |

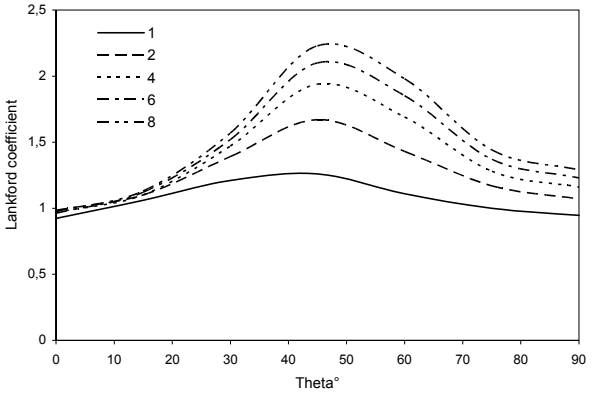


***Figure 3:*** *T_Pyramidal effect with ALAMEL model (with T_prismatic=1.2 and 1/m=30)*

The strain rate sensitivity has also an effect on the Lankford coefficient. When it increases from 5 to 30, there is low effect at 0° (+1.16%), r increases by 17.36% at 45° and by 9.32% at 90°.

### 4.2 SUMMARY AND COMPARISON WITH EXPERIMENTAL RESULTS:

Table 2 summarises the effects of the variations the critical resolved shear stresses (prismatic and pyramidal) and the strain rate sensitivity on the Lankford coefficient.

By using different values of CRSSs and strain rate sensitivity in these simulations, the best results (compared to experimental results) are obtained with the PSD and the PCK model with the values described in Table 3.

Experimental results, given in the investigations of Fundenberger [6] and M. Preilla & G. Sevillano [7], and the optimal results obtained with the parameters in Table 3 are illustrated in the Figure 4.

***Table 3***: *Optimal values of CRSSs and S.R. sensitivity approaching experimental values of the Lankford coefficient*

| Model | PSD | PCK |
|---|---|---|
| T_PRISM | 1 | 0.2 |
| T_PYRAM | 8 | 8 |
| Strain rate sensitivity (1/m) | 20 | 5 |

## 5 CONCLUSIONS

A sensitivity study of the Lankford coefficient to the critical resolved shear stresses and to the strain rate sensitivity (1/m) was performed for the TA6V alloy. The dependence of the Lankford coefficient on the T_pyramidal is shown for all used models. However the model used (relaxation, grain shape) has a large influence on the results.

Using these study results and a new experimental campaign where texture, grain shape, Lankford coefficients, yield stresses and hardening value are measured, a new identification is currently going on.

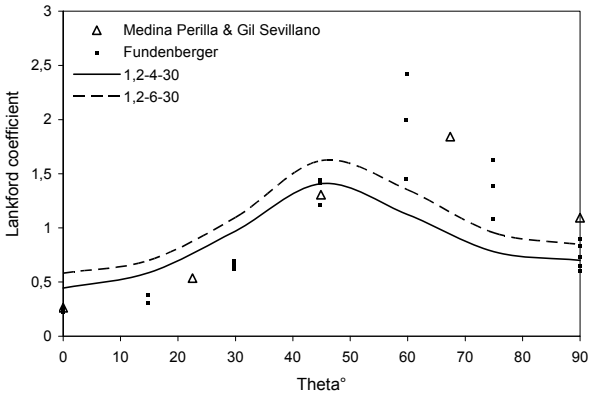


***Figure 4:*** *Optimal results (with the parameters of Table 3) compared to experimental values of the Lankford coefficient.*

## ACKNOWLEDGEMENT

The authors acknowledge the Interuniversity Attraction Poles Programme - Belgian State – Belgian Science Policy (Contract P6/24). The Belgian Fund for Scientific Research FRS-FNRS is also acknowledged.

## REFERENCES

[1] Delannay, L., Loge, R.E., Chastel, Y., Van Houtte, P. Prediction of intergranular strains in cubic metals using a multisite elastic–plastic model. Acta Mater. 50: 5127–5138 (2002).

[2] Van Houtte, P., Li, S., Seefeldt, M., Delannay, L.: Deformation texture prediction: from the Taylor model to the advanced Lamel model. International Journal of Plasticity 21: 589-624 (2005).

[3] M.J. Phillippe, M. Serghat, P. Van Houtte & C. Esling. Modelling of texture evolution for materials of hexagonal symmetry -II applications to zirconium and titanium α or near α alloys, Acta Metallurgica & Materialia, 43: 1619-1630, 1995.

[4] G. Lütjering, J.C. Williams, Titanium, Springer, Second edition.

[5] J.R. Mayeur, D.L. McDowell. A three-dimensional crystal plasticity model for duplex Ti-6Al-4V. International journal of plasticity, 23, 1457-1485, 2007.

[6] J. J. Fundenberger, M. J. Philippe, F. Wagner and C. Esling, Modelling and prediction of mechanical properties for materials with hexagonal symmetry (Zinc, Titanium and Zirconium alloys), Acta Metallurgica et Materialia, , 45(10), 4041-4055, 1997.

[7] J.A. Medina Perilla, J. Gil Sevillano, Two-dimensional sections of the yield locus of a Ti-6Al-4V alloy with a strong transverse type crystallographic α texture, Materials science and engineering, A201, 103-110, 1995.